Catalysis Communications 58 (2015) 122–126

Contents lists available at ScienceDirect

Catalysis Communications

journal homepage: www.elsevier.com/locate/catcom

Short Communication

BiOCl nanosheet/$Bi_4Ti_3O_{12}$ nanofiber heterostructures with enhanced photocatalytic activity

Mingyi Zhang, Ying Liu, Lu Li, Hong Gao, Xitian Zhang *

Key Laboratory for Photonic and Electronic Bandgap Materials, Ministry of Education, School of Physics and Electronic Engineering, Harbin Normal University, Harbin 150025, People's Republic of China

ARTICLE INFO

Article history:
Received 16 July 2014
Received in revised form 8 September 2014
Accepted 10 September 2014
Available online 19 September 2014

Keywords:
BiOCl
$Bi_4Ti_3O_{12}$
Heterostructure
Photocatalysis
Degradation

ABSTRACT

Aurivillius oxide semiconductors are important photocatalyst because of their unique electronic structure and layered crystal. In this paper, two kinds of Aurivillius oxide semiconductors heterostructures based on $Bi_4Ti_3O_{12}$ nanofibers frameworks and BiOCl nanosheets are successfully synthesized by combining the electrospinning technique and solvothermal method. The high-resolution transmission electron microscopy results reveal that an intimate interface between $Bi_4Ti_3O_{12}$ nanofibers and BiOCl nanosheets forms in the heterojunctions. Photocatalytic tests show that the BiOCl/$Bi_4Ti_3O_{12}$ heterostructures exhibit enhanced photocatalytic activity than bare $Bi_4Ti_3O_{12}$ and BiOCl, mainly owing to the photoinduced interfacial charge transfer based on the photosynergistic effect of the BiOCl/$Bi_4Ti_3O_{12}$ heterojunction. At the end, the photocatalytic mechanism with $\bullet O_2^-$ production was studied.

1. Introduction

Heterogeneous photocatalysis by semiconductor materials has become an exciting and rapidly growing area of research in the last few years. It can be used to decompose organic compounds into inorganic matter for the purpose of water purification, and to release hydrogen from water for clean energy generation [1–6]. Recently, bismuth oxychloride (BiOCl), as a novel photocatalyst, has attracted much attention due to its excellent photocatalytic properties. It is reported that nanostructured BiOCl exhibits better performance than TiO_2 (P25, Degussa) for the photocatalytic degradation of methyl orange (MO) dye [7–11]. However, the same problems existed for the application of BiOCl to those of TiO_2 photocatalyst: (1) BiOCl can utilize only the photons in the wavelength shorter than 380 nm, which occupies no more than 4% of the solar spectrum. (2) The rapid recombination of photoinduced electrons and holes greatly lowers the quantum efficiency [12]. (3) For those nanostructured BiOCl, the separation rate of photoinduced surface and volume charge carriers in a photocatalyst can be significantly increased by reducing its size to the appropriate nanoscale level, however, the recycling of the photocatalysts hinders their applications due to their small size. Therefore, it is of great interest to design efficient and practical visible light driven BiOCl photocatalysts with excellent charge separation characteristics and favorable recycling capabilities.

The manipulation of semiconductor heterostructures is one of the effective methods for photoinduced electron–hole generation and separation [13–16]. Compared to a single semiconductor, coupling of BiOCl with other narrow band-gap semiconductors forming a junction structure has been found to enhance the photocatalytic performance, because multiple semiconductors can absorb a larger fraction of the solar spectrum, which is beneficial for the excitation of the semiconductor and thus the photoinduced generation of electrons and holes. Moreover, the coupling of two different semiconductors could transfer electrons from an excited small band gap semiconductor into another attached one in the case of proper conduction band potentials. This favors the separation of photoinduced electrons and holes and thus improves the photocatalytic efficiency of the semiconductor heterostructure dramatically.

Based on the above considerations, in this work we report a successful attempt for the fabrication of the BiOCl/$Bi_4Ti_3O_{12}$ hierarchical heterostructures based on $Bi_4Ti_3O_{12}$ nanofibers via a simple electrospinning technique and solvothermal method (Scheme S1). $Bi_4Ti_3O_{12}$ and BiOCl both belong to the same layered Aurivillius oxide family with strong absorption in the visible light region. $Bi_4Ti_3O_{12}$ and BiOCl all consisting of $[Bi_2O_2]^{2+}$ layers (*X–Bi–O–Bi–X*) are sandwiched between two slabs of *X* ions, atoms or groups (where X = $Bi_2Ti_3O_{10}^{2-}$ and Cl^-). They can easily grow together to form heterostructures through an ion exchange process [17]. The experimental results show that the as-obtained BiOCl/$Bi_4Ti_3O_{12}$ photocatalysts exhibited excellent photocatalytic activity. The mechanisms for the photocatalytic degradation of MO and 4-NP over the BiOCl/$Bi_4Ti_3O_{12}$ hierarchical heterostructures are discussed in detail. Moreover, due to the large length-to-diameter

* Corresponding author.
E-mail address: xtzhangzhang@hotmail.com (X. Zhang).

http://dx.doi.org/10.1016/j.catcom.2014.09.021
1566-7367/

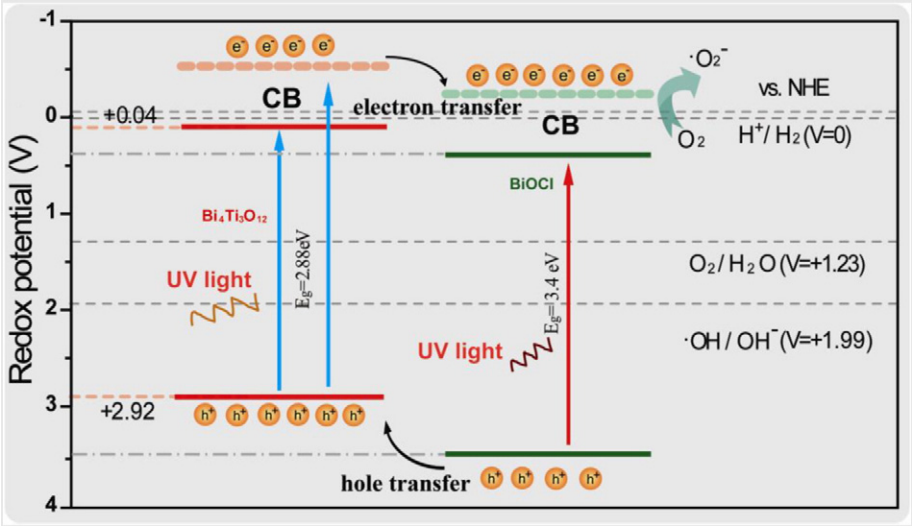

Scheme 1. Schematic of the band structures of BiOCl/$Bi_4Ti_3O_{12}$ heterostructures and possible electron–hole separations.

ratio of the $Bi_4Ti_3O_{12}$ nanofibers, the BiOCl/$Bi_4Ti_3O_{12}$ heterostructure photocatalysts can be recovered easily by sedimentation without a decrease in the photocatalytic activity.

2. Experimental

For the sample preparation, characterization and photocatalytic test see the Experimental section in the Supporting Information.

3. Results and discussions

Fig. 1 shows the XRD pattern of the $Bi_4Ti_3O_{12}$ nanofibers and BiOCl/$Bi_4Ti_3O_{12}$ heterostructures. As shown in Fig. 1, the main diffraction peaks of the BTO nanofibers can be indexed to the orthorhombic $Bi_4Ti_3O_{12}$ (JCPDS no. 8-258). No peaks of impurities can be observed, demonstrating the high phase purity of the as-prepared $Bi_4Ti_3O_{12}$ nanofibers. As for the BiOCl/$Bi_4Ti_3O_{12}$ heterostructures, except the diffraction peaks of $Bi_4Ti_3O_{12}$, the diffraction peaks of BiOCl are also clearly

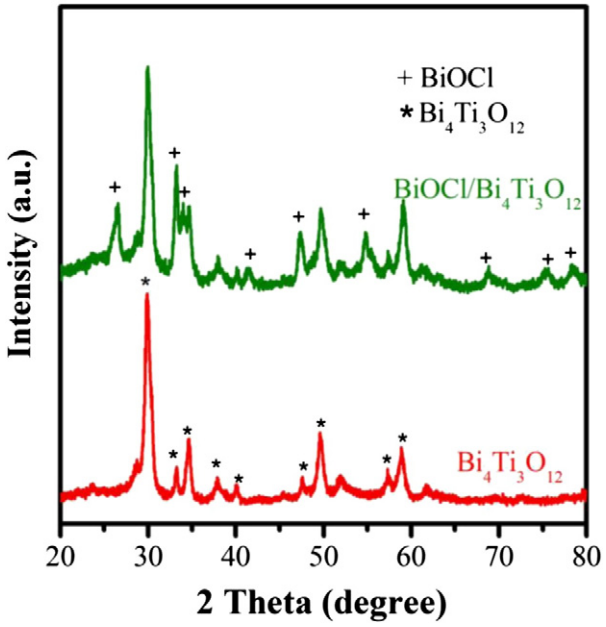

Fig. 1. XRD patterns of the samples.

observed corresponding to the (131), (200), (152), (331) and (262) crystal planes of koechlinite BiOCl (JCPDS no. 21-0102). These results suggest that the BiOCl has been formed on the $Bi_4Ti_3O_{12}$ nanofibers by solvothermal processing.

Fig. S1 shows the FESEM image of $Bi(NO_3)_3$–TBT–PVP nanofibers which are fabricated by electrospinning. It can be clearly seen that the nanofibers are of a relatively smooth surface with a diameter of around 150 nm. Fig. 2a and b displays the FESEM images for the products that were obtained by annealing the as-spun $Bi(NO_3)_3$–TBT–PVP nanofibers at 550 °C. The $Bi_4Ti_3O_{12}$ nanofibers have a very smooth surface and the diameters reduce to an average diameter of 80 nm compared to the as-spun nanofibers, resulting from the decomposition of $Bi(NO_3)_3$, TBT and PVP. Fig. 2c shows a typical SEM image of the as-synthesized BiOCl/$Bi_4Ti_3O_{12}$ hierarchical heterostructures, where the $Bi_4Ti_3O_{12}$ nanofibers are fully decorated with uniform BiOCl nanosheets. The nanosheets are evenly distributed across the entire surface of each nanofiber and connected to each other, forming a network of relief features on the rough surface of each $Bi_4Ti_3O_{12}$. From the image shown in Fig. 2d, it is easy to observe that the BiOCl nanosheets are in fact very thin flakes with an average thickness of about 10 nm and an average edge length of about 50–100 nm. Additionally, the EDX spectrum (Fig. S2) confirms the presence of C, O, Bi, Ti and Cl elements in the hierarchical heterostructures. In addition, the EDX analysis indicates that the atomic ratio of Ti to Cl is 1:4 for the hierarchical heterostructures. Fig. 2e shows the typical TEM images of BiOCl/$Bi_4Ti_3O_{12}$ hierarchical heterostructures. It can be seen that the $Bi_4Ti_3O_{12}$ nanofiber is composed of nanoparticles, and each nanoparticle attaches to several other nanoparticles. Many pores are observed within the spaces between adjacent nanoparticles. The TEM images reveal that BiOCl nanosheets are coated around the primary $Bi_4Ti_3O_{12}$ nanofiber, coinciding with the results from the FESEM observations. The HRTEM image from two hierarchical heterostructures all display two types of clear lattice fringes as shown in Fig. 2f. The fringe observed in Fig. 2f corresponds to the interplanar distance of 0.33 nm, which agrees well with the lattice spacing of the (151) plane of the $Bi_4Ti_3O_{12}$ nanofiber. In addition, the spacing between the adjacent lattice fringes is 0.34 nm, corresponding to the *d*-spacing of the (101) plane of the BiOCl nanosheet. The HRTEM images clearly exhibit that the as-adopted fabrication route to realize a close contact of BiOCl nanosheets with $Bi_4Ti_3O_{12}$ nanoparticles in the BiOCl/$Bi_4Ti_3O_{12}$ hierarchical heterostructures is successful. Such close contact is very beneficial to the separation of photogenerated electron–hole pairs in the process of photocatalytic reaction.

Fig. S3 shows nitrogen adsorption–desorption isotherms of BiOCl/$Bi_4Ti_3O_{12}$ hierarchical heterostructures and corresponding pore